Article

Heat Transfer Potential of Unidirectional Porous Tubes for Gas Cooling under High Heat Flux Conditions

Kazuhisa Yuki [1,*]**, Risako Kibushi** [1]**, Ryohei Kubota** [1]**, Noriyuki Unno** [1]**, Shigeru Tanaka** [2] **and Kazuyuki Hokamoto** [2]

[1] Department of Mechanical Engineering, Tokyo University of Science, Yamaguchi 1-1-1 Daigakudori, Sanyo-Onoda 756-0884, Japan; kibushi@rs.socu.ac.jp (R.K.); f118025@ed.socu.ac.jp (R.K.); unno@rs.socu.ac.jp (N.U.)

[2] Institute of Industrial Nanomaterials, Kumamoto University, 2-39-1 Kurokami, Chuo-ku, Kumamoto 860-8555, Japan; tanaka@mech.kumamoto-u.ac.jp (S.T.); hokamoto@mech.kumamoto-u.ac.jp (K.H.)

* Correspondence: kyuki@rs.socu.ac.jp

Abstract: To discuss a suitable porous structure for helium gas cooling under high heat flux conditions of a nuclear fusion divertor, we first evaluate effective thermal conductivity of sintered copper-particles in a simple cubic lattice by direct numerical heat-conduction simulation. The simulation reveals that the effective thermal conductivity of the sintered copper-particle highly depends on the contacting state of each particle, which leads to the difficulty for the thermal design. To cope with this difficulty, we newly propose utilization of a unidirectional porous tube formed by explosive compression technology. Quantitative prediction of its cooling potential using the heat transfer correlation equation demonstrates that the heat transfer coefficient of the helium gas cooling at the pressure of 10 MPa exceeds 30,000 W/m^2/K at the inlet flow velocity of 25 m/s, which verifies that the unidirectional porous copper tubes can be a candidate for the gas-cooled divertor concept.

Keywords: unidirectional porous tube; gas cooling; high heat flux condition; fusion reactor; divertor; effective thermal conductivity; sintered particles; porous media

1. Introduction

The surrounding of the core plasma in a fusion reactor contains structures and equipment exposed to extremely severe heat loads, such as the first wall and the divertor. These must withstand the radiation from the plasma and the load of high energy particles while continuously maintaining these functions. For example, the divertor, to which α-particles flow directly, is subjected to a localized, but steady, heat load of about 10 MW/m^2. It goes without saying that in such an extreme thermal load environment, a sufficient cooling margin is essential but, at the same time, the establishment of a thermal design with excellent economic efficiency, soundness, and maintainability is the key for the realization of nuclear fusion power reactors.

Based on the above background, the development of the divertor cooling technology is one of the most important issues of the reactor engineering. In ITER (International Thermonuclear Experimental Reactor), which is currently under construction in Cadarache, France, a water-cooled system is adopted for the divertor cooling because of the emphasis on self-ignition and demonstration of the reactor engineering technologies. To enhance the cooling performance, a swirl tube with an inserted twisted tape is applied [1,2]. As the fluid flows in the swirl tube while turning spirally, a secondary flow is formed by centrifugal force. In this way, fluid mixing is promoted, resulting in thinning the temperature boundary layer and improving the cooling performance, as well as the increase in the critical heat flux. On the other hand, the application of screw tubes with a threaded structure on the inner surface of the tube has been studied in the divertor of JT-60SA and the prototype

reactor [3,4]. The cooling performance of the screw tube proved higher than that of the swirl tube with the same pumping power because of the effect of increased heat transfer area and fluid stirring in the vicinity of the tube wall. As another water-cooling technique for the divertor, Toda has proposed an ultra-low flowrate-type evaporative heat transfer device, EVAPORON (Evaporated Fluid Porous Thermodevice), which utilizes the latent heat of vaporization of a cooling liquid in a metal porous medium [5]. Furthermore, the author has upgraded it to EVAPORON-2, which is equipped with subchannels for enhancement of vapor discharge and has demonstrated cooling performance exceeding 20 MW/m^2 at extremely low flow rates [6,7]. So far, the authors have also proposed EVAPORON-3 [8], adaptable to large divertor surfaces, and EVAPORON-4 [9], which applies a unidirectional porous medium.

In recent years, however, the helium gas cooling has been reconsidered as a highly safe cooling method for divertors [10–12]. In particular, international joint research had been conducted as one of the tasks of PHOENIX, the Japan/U.S. fusion research collaboration project. To apply helium, which has a low heat capacity, as a coolant, the HEMJ (Helium-cooled Multi-Jet) cooling method has been studied, in which helium is compressed up to about 10 MPa and injected as an impinging jet flow into a narrow channel equipped with a number of nozzles [13]. Although a heat transfer coefficient exceeding 30,000 W/m^2/K has been obtained at the pressure of 10 MPa, deterioration of the heat transfer performance due to re-laminarization has also been pointed out [14].

To complement the low heat transfer performance of the gas cooling, it is necessary to introduce a cooling technology that encompasses all the technologies related to heat transfer enhancement, such as (1) increasing the heat transfer area, (2) promoting turbulent heat transfer, and (3) utilizing micro- and mini-channels. We can know various kinds of heat transfer promoters for the gas flow from Tao's review article [15]. From the viewpoint of high heat flux conditions that needs extremely high heat transfer coefficient, the cooling technology using porous media is the one that satisfies all of the above criteria. In the existing studies for the divertor cooling, Hermsmeyer et al. theoretically demonstrated that the heat transfer coefficient of the helium gas flow in pin fin porous arrays exceeds 60,000 W/m^2/K at the inlet flow velocity of 20 m/s (averaged local velocity: 120 m/s) and the pressure of 10 MPa [16]. Sharafat et al. focused on the cooling technique that uses metal foam and his CFD simulation verified that the heat transfer coefficient is in the range from 12,500 to 25,000 W/m^2/K for the modeled flow at the inlet flow velocity of 150 m/s and the pressure of 4 MPa [17,18]. Yuki et al. studied the cooling performance using sintered particles and the heat transfer coefficient of N$_2$ gas impinging jet flow with the porous medium is much higher than that of common impinging jet flow without the porous medium from the viewpoint of not only flow velocity, but also pumping power [19]. Up to now, however, the issue of a porous medium suitable for cooling the high heat flux of the divertor has not been sufficiently addressed. Toward the optimal control of the porous structure for the high heat flux removal, 3D-printed porous metals fabricated by selective laser metal melting (SLMM) technology, such as a porous lattice [20], are also candidates. Various kinds of the 3D-printed porous metal [21–25] can be expected to bring out the heat transfer potential because we can easily control the porosity and pore size distribution against the heat load and cooling conditions. However, the fabrication of a 3D-printed porous "copper" with micro/mini channels seems to be considerably difficult in the conventional 3D-printed technology.

Against these backgrounds, in this study, we first focus on again the pros and cons of utilizing sintered copper-particles porous media with excellent thermal conductivity and vast heat transfer surface from the viewpoint of the high heat flux removal. After that, we newly propose the introduction of a unidirectional porous tube formed by explosive compression technology, which was developed by Hokamoto et al. [26], and demonstrate its cooling potential by the heat transfer correlation equation constructed by the author's heat transfer experiments.

2. Prediction of Effective Thermal Conductivity of Sintered Copper-Particles by Direct Numerical Simulation of Heat Conduction

2.1. Procedure for Evaluating Effective Thermal Conductivity of Porous Medium

A general formula for estimating the effective thermal conductivity k_{eff} [W/m/K] of porous media is shown as follows:

$$k_{\text{eff}} = \varepsilon k_{\text{f}} + (1 - \varepsilon)k_{\text{s}} \tag{1}$$

where, ε is the porosity, and k_{f} [W/m/K] and k_{s} [W/m/K] are the thermal conductivities of the fluid and the porous solid, respectively. Although Equation (1) indicates that the effective thermal conductivity is solely based on the porosity of the porous media, a highly versatile correlation equation for the effective thermal conductivity should be taken into account using the porosity, the pore size, the structure, and other parameters that affect the effective thermal conductivity (e.g., thermal contact resistance between particles, etc.).

For that purpose, in this study, the effective thermal conductivity is directly evaluated using a three-dimensional numerical simulation of heat conduction inside the porous medium. Here, we focus on sintered copper-particles as the porous media because the sintered particles have higher thermal conductivity compared to other porous media.

Figure 1 shows the simulation model to evaluate the effective thermal conductivity. The porous medium is a structure in which the sphere particles are placed in a simple cubic lattice, which is assumed to have the highest effective thermal conductivity among all means of placing the particles. The particles, 1.0 mm in diameter, are packed by placing five pieces along the horizontal, vertical, and lateral sides, making the size of the formed porous medium $5 \times 5 \times 5$ mm (see Figure 1 on the right). The porosity ε for this structure is 0.48. Figure 1 on the right shows the method for jointing the sphere particles. To reproduce a porous bed in which the sphere particles are sintered or point-contacted, the particles are joined by a cylinder having a diameter d [mm], which is determined by the central angle θ [°] of the particles (hereafter, contact angle). Square rods, 5.0 mm wide and 50 mm long, are attached to the upper and lower parts of the porous medium. A square plate of 1.0 mm in thickness is attached to the upper surface of the rod 2 to set a constant temperature during the simulation. The finite element method is used for solving the 3-dimentional equation of the heat conduction. We utilized a commercial software "CreoParametric ver.6.0" for the simulation. Pure copper with thermal conductivity k_{s} = 398 W/m/K is set for all solid parts of the simulation model. The void portion of the porous bed is filled with a static air (thermal conductivity k_{f} = 0.0256 W/m/K). As for the boundary conditions, all the side walls are defined as adiabatic conditions, the heat flux of 500,000 W/m^2 is uniformly applied to the bottom surface of the rod 1, and the top surface of the rod 2 is set to 100 °C. The most important parameter in this simulation is the contact angle θ formed between the particles. There are six patterns: θ = 5°, in which the particles are close to point contact; and θ = 10°, 20°, 30°, 40°, and 50°, close to the state in a sintered particle. Before the simulation, the suitable mesh size and structure were sufficiently evaluated and discussed many times especially in the contacting region of the particles. The effective thermal conductivity k_{eff} [W/m/K] of the sintered copper-particles is estimated on the basis of the temperature difference T_1–T_2 obtained by the simulation, as follows:

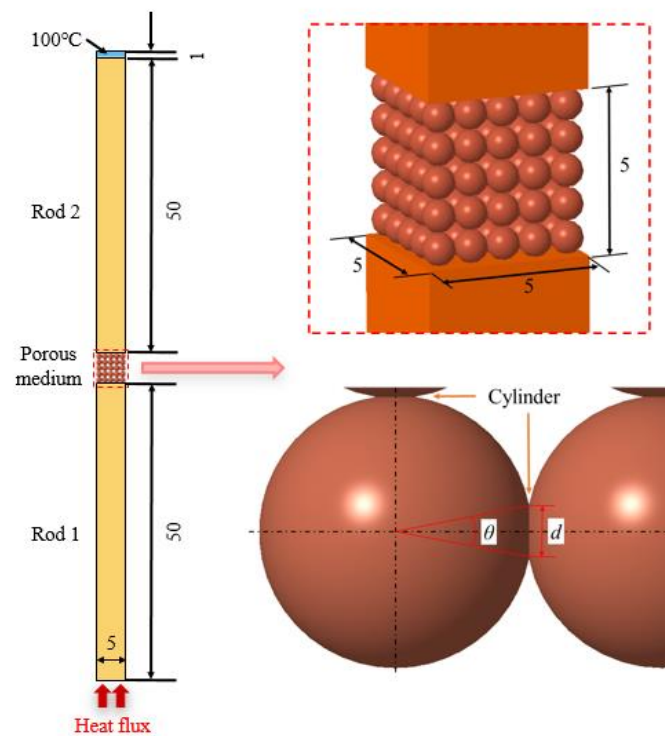$$k_{\text{eff}} = \frac{q \times \Delta y}{T_1 - T_2} \tag{2}$$

Figure 1. Simulation model for evaluating effective thermal conductivity.

In this equation, q [W/m^2] is the heat flux, Δy [m] is the length of the porous bed in the y-direction, and T_1 [K] and T_2 [K] represent the temperatures of the joint surface between the rod 1 or rod 2 and the porous bed, respectively. These temperatures are determined by approximating the temperature distribution in the rods as a linear function using the least squares method, where the temperature distribution in the axial direction can be regarded as one-dimensional profile. This evaluation method of the thermal conductivity is well-known as the steady method (experimental method).

2.2. Effective Thermal Conductivity of Sintered Copper-Particles

Figure 2 shows the effective thermal conductivity for each contact angle. The value (%) in the figure is the ratio of the effective thermal conductivity to the thermal conductivity of pure copper. According to the results of the simulation, the effective thermal conductivities are 15.1, 27.5, 49.8, 72.0, 93.6, and 114.6 W/m/K for the contact angles $\theta = 5°$, $10°$, $20°$, $30°$, $40°$, and $50°$ respectively. This clearly verifies that the effective thermal conductivity increases with increasing contact area (i.e., the degree of sintering). Compared to the thermal conductivity of pure copper, if the contact area between the particles is small (i.e., the contact angle $\theta = 5°$, which is a state close to point contact), the effective thermal conductivity is reduced to 3.8% of that of pure copper, whereas even at $\theta = 50°$, simulating a sufficiently sintered state, the thermal conductivity of copper is reduced to approximately 29%. These results indicate that less than 30% of the thermal conductivity of pure copper can be utilized even with a simple cubic lattice, which has the highest effective thermal conductivity among different particle placements. Furthermore, it is worth mentioning that the effective thermal conductivity estimated by the porosity weighting Equation (1) is significantly different from the simulation results and overestimates the effective thermal conductivity when the thermal conductivity of the porous solid, k_s, is given as that of pure copper. This demonstrates that the porosity information is not sufficient for calculating the effective thermal conductivity and that a correlation equation that reflects the tortuosity of the porous media, i.e., packing structure of the particles and the degree of sintering, is required.
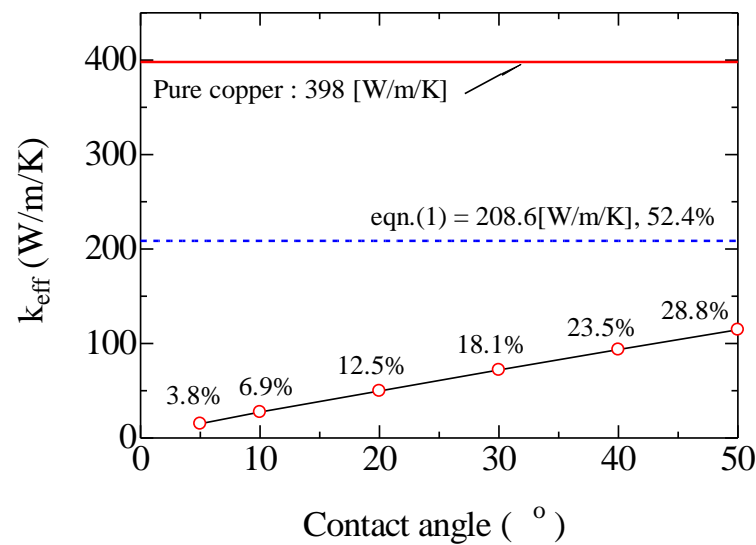
Figure 2. Effective thermal conductivity of copper sintered particle.

Furthermore, these results verify that, even in the case of placing the particles in a certain cubic lattice, the optimal design for the heat transfer enhancement must take into account the actual effective thermal conductivity of the sintered copper-particle, as well as the thickness of the porous layer to increase the fin efficiency, etc. In addition, the contacting state between the particles, as well as between the particle-sintered porous medium and the heat transfer surface, highly affects the fin effect inside the porous medium, which makes it more difficult to precisely predict the cooling performance of forced convective heat transfer using the sintered copper-particle. Especially under high heat flux conditions such as nuclear fusion divertors, precise evaluation of the effective thermal conductivity highly affects the prediction of the surface temperature of an armor material of the divertor that faces the core plasma.

3. Heat Transfer Potential of Unidirectional Porous Copper Tube of Gas Flow

Heat Transfer Correlation of Gas Flow in Unidirectional Porous Tubes Fabricated by Explosive Compression Technology

To cope with the difficulty of precise thermal design using the sintered copper-particle porous media for the divertor cooling, we focus on completely new porous copper tubes with uniformly-distributed pore holes fabricated by explosive compression technique that was developed by Hokamoto et al. [26]. This unique unidirectional porous tube (hereafter, porous tube) is fabricated by compressing a bundle of thin copper tubes by a gunpowder explosion that is set around the bundle (see Figure 3). One of the features of the porous tube is high thermal conductivity, even in the radial direction. For instance, the effective thermal conductivities of the porous tube in the axial and radial directions ($k_{\mathrm{eff}//}$ and $k_{\mathrm{eff}\perp}$) are approximately 210 W/m/K and 110 W/m/K at the porosity of 50 %, respectively, which enables active utilization of the vast heat transfer surface of the porous tube. Here, $k_{\mathrm{eff}//}$ can be estimated by Equation (1) and $k_{\mathrm{eff}\perp}$ is based on the Ogushi's equation [27].

$$k_{\mathrm{eff}\perp} = \frac{(\beta+1)+\varepsilon(\beta-1)}{(\beta+1)-\varepsilon(\beta-1)}k_s \tag{3}$$
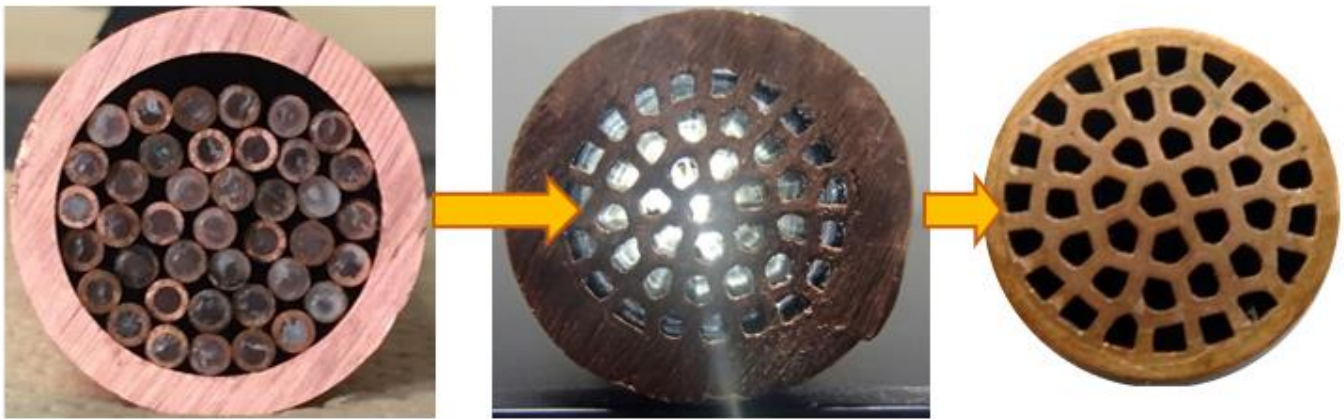
Figure 3. Unidirectional porous copper tube #1 (before and after explosive compaction).

Figure 4 shows a high fin efficiency of the unidirectional porous plate fins (1.0 mm × 10 mm × 10 mm), compared to that of a sintered copper-particle fin (Each porosity is 50%). In addition, the pore diameter and the porosity can be optionally adjustable by changing the thin copper tube with different inner diameter and thickness. Utilizing the porous tube as a heat transfer promoter also makes it possible to reduce the pressure loss in comparison with other porous media such as a sintered particle because of its unidirectional pore structure. As the result, the porous tube also enables to reduce the pumping power.
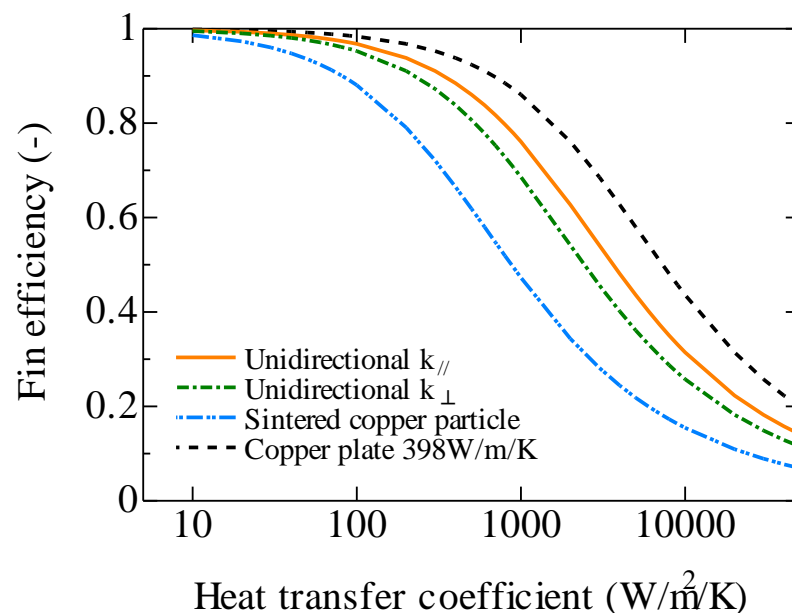

Figure 4. Fin efficiency of sintered copper-particle and unidirectional porous copper.

In past studies regarding the unidirectional porous tube, Fiedler et al. evaluated the mechanical and thermal properties [28]. Regarding the heat transfer characteristics of the unidirectional porous copper tube, the author firstly demonstrated its extremely high heat transfer performance for gas flow [29,30]. In addition, Kibushi et al. [31] evaluated the heat transfer characteristics of many kinds of the porous tubes as shown in Table 1. The heat transfer experiments were performed using a double-tube heat exchanger, where the porous tube is set as the inner tube. Hot water flows inside the annular channel between the outer tube and the porous tube, and air driven by the compressor flows through the porous tube. As to the details of the heat transfer experiments, please see reference [31]. The experimental results clarified that the heat transfer performance of the porous tubes is

7.4 times higher than that of the circular tube flow at the maximum and superior compared with other heat transfer promoter tubes such as the swirl tube and artificially roughened ducts (see Figure 5). Furthermore, we constructed a heat transfer correlation equation.

Table 1. Specifications of porous tubes.

	#1	#2	#3	#4	#5	#6
Length (mm)	470	455	340	475	450	440
Number of pore	40	40	40	21	13	9
Pore size (mm)	1.69	2.16	2.71	2.60	3.51	4.61
Porosity (%)	35.5	57.7	81.3	44.2	49.5	59.1
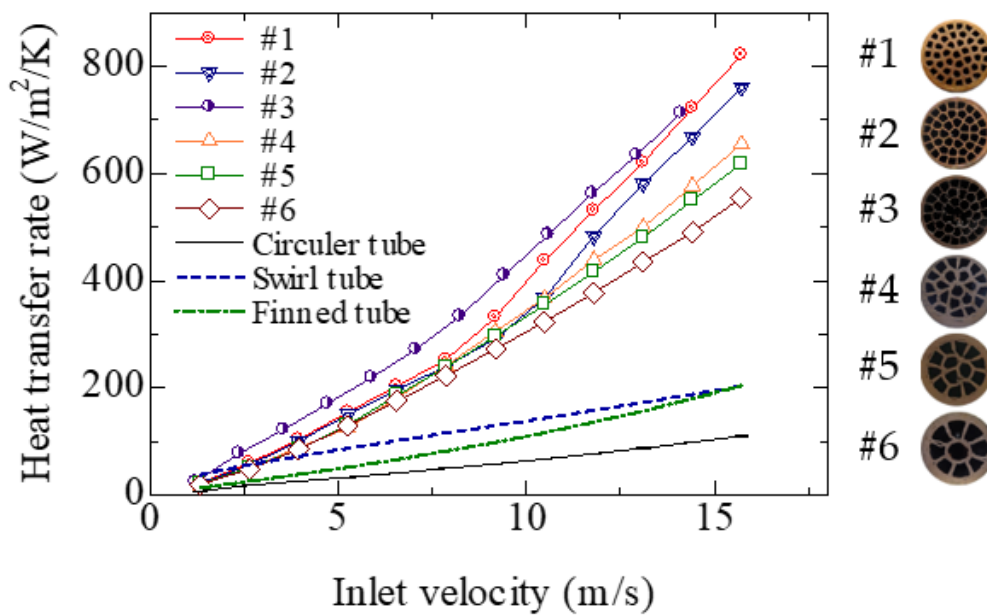
Figure 5. Heat transfer performance of porous tubes.

Of course, the demonstration experiment of the porous tube toward the heat transfer coefficient of 30,000 W/m^2/K at least, should be carried out under the divertor cooling conditions using helium flow, but the experimental demonstration is considerably difficult because the pressure is extremely high, approximately 10 MPa, and the temperature of the helium flow is higher than 300 °C. In that sense, the heat transfer potential should be evaluated instead, as the first step, by applying the following heat transfer correlation equation of the porous tube flow we constructed in reference [31].

$$Nu = 0.286\,Re^{0.8}Pr^{0.4}\left(\frac{d_{\text{pore}}}{D}\right)^{-0.388}\left(\frac{k_{\text{eff}}}{k_{\text{gas}}}\right)^{-0.176} \tag{4}$$

Here, $Nu = hD/k_{\text{gas}}$ (k_{gas}) is thermal conductivity of gas, and D is inside diameter of the porous tube [m]). The porous copper tube has long and unidirectional pore structure, therefore, the heat transfer correlation equation is constructed based on the Dittus-Boelter correlation equation, which is a well-known correlation for turbulent convective heat transfer in a circular tube. In addition, the correlation equation for the porous tubes takes into account the pore structure as the ratio of the pore size d_{pore} to the tube diameter D, and the effective thermal conductivity as the ratio of the effective thermal conductivity of the porous tube k_{eff} to the thermal conductivity of the gas k_{gas}. Here, the effective thermal conductivity of the porous copper tubes k_{eff} is calculated using the Equation (3).

Here, the heat transfer coefficient of the helium gas flow in the porous copper tube is predicted using the physical property of the helium gas at the temperature of 300 °C

and the pressure of 10 MPa. The porous tube #1 in Table 1, which showed the highest heat transfer performance in Figure 5, is used for the potential evaluation, because the porous tube with thicker solid wall is more suitable for achieving the high heat transfer coefficient from the viewpoint of the fin theory. Figure 6 shows the predicted heat transfer performance of the helium gas flow. The heat transfer coefficient exceeds 30,000 W/(m²·K) at the inlet flow velocity of 25 m/s (average velocity in each pore is 70.4 m/s). In addition, the heat transfer coefficient of over 30,000 $W/m^2/K$ could easily be possible by optimizing the pore size and the porosity of the porous tube, which indicates that the porous copper tubes can be one of candidates for the gas-cooled divertor concept. As to the pressure loss, we can apply the Darcy–Weisbach equation, which is commonly utilized for the pressure loss prediction of a circular tube flow, depending on the actual piping geometry for the divertor cooling, because the unidirectional porous tube is an assembly of circular tubes (if there is no deformation of the inner thin tube).
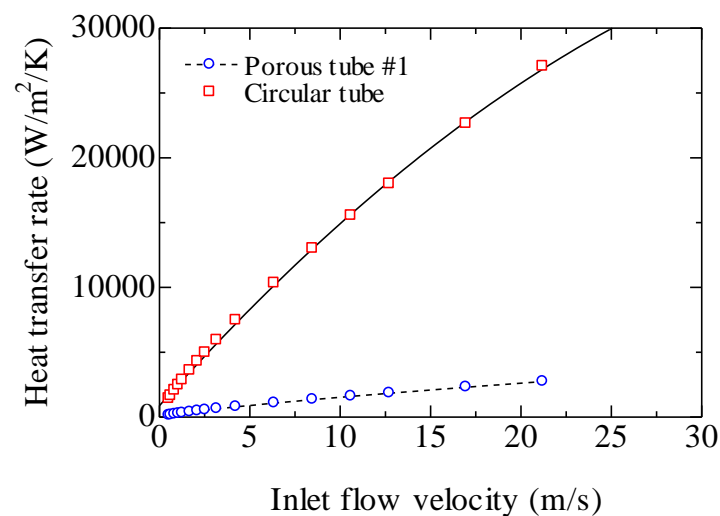

Figure 6. Heat transfer performance of helium gas flow in unidirectional porous tube.

4. Conclusions

To discuss suitable porous structure for gas-cooled divertor concept under high heat flux conditions of 10 MW/m^2, we first evaluated effective thermal conductivity of sintered copper-particle in a simple cubic lattice by direct numerical heat-conduction simulation. The simulation revealed that the effective thermal conductivity of the sintered copper-particle is in the range from 15.1 to 114.6 W/m/K (pure copper: 398 W/m/K) and highly depends on the contacting state of the particles, which makes it difficult to predict the exact temperature of divertor armor material. To cope with this difficulty, we newly proposed the utilization of a unidirectional porous copper tube formed by explosive compression technology. As the experimental demonstration is considerably difficult under the divertor cooling conditions, quantitative prediction of its cooling potential using the heat transfer correlation equation proved that the heat transfer coefficient of the porous tube with the porosity of 35.5% and the averaged pore size of 1.69 mm exceeds 30,000 $W/m^2/K$ at the inlet flow velocity of 25 m/s and the pressure of 10 MPa, which verifies that the porous copper tubes can be one of candidates for the gas-cooled divertor concept.

References

1. Raffray, A.R.; Schlosser, J.; Akiba, M.; Araki, M.; Chiocchio, S.; Driemeyer, D.; Escourbiac, F.; Grigoriev, S.; Merola, M.; Tivey, R. Critical heat flux analysis and R&D for the design of the ITER divertor. *Fusion Eng. Des.* **1999**, *45*, 377–407.
2. Araki, M.; Sato, K.; Suzuki, S.; Akiba, M. Critical-heat-flux experiment on the screw tube under one-sided-heating conditions. *Fusion Technol.* **1996**, *29*, 519–528. [CrossRef]
3. Boscary, J.; Araki, M.; Suzuki, S.; Ezato, K.; Akiba, M. Critical heat flux in subcooled water flow of one-side-heated screw tubes. *Fusion Technol.* **1999**, *35*, 289–296. [CrossRef]
4. Ezato, K.; Suzuki, S.; Sato, K.; Akiba, M. Thermal fatigue experiment of screw cooling tube under one-sided heating condition. *J. Nucl. Mater.* **2004**, *329*, 820–824. [CrossRef]
5. Toda, S.; Ebara, S.; Hashizume, H. Development of an advanced cooling device using porous media with active boiling flow counter to high heat flux. Fundamental study on high heat flux removal system using evaporated fluid in metal porous media. In Proceedings of the 11th International Heat Transfer Conferences (IHTC11), Kyongju, Korea, 23–28 August 1998; pp. 503–508.
6. Yuki, K.; Hashizume, H.; Toda, S. Sub-channels-inserted porous evaporator for efficient divertor cooling. *Fusion Sci. Technol.* **2011**, *60*, 238–242. [CrossRef]
7. Yuki, K.; Hashizume, H.; Toda, S.; Sagara, A. Divertor cooling with sub-channels-inserted metal porous media. *Fusion Sci. Technol.* **2013**, *64*, 325–330. [CrossRef]
8. Takai, K.; Yuki, K.; Sagara, A. Heat transfer performance of EVAPORON-3 developed for an enlarged heat transfer surface of divertor. *Plasma Fusion Res.* **2017**, *12*, 1405015. [CrossRef]
9. Takai, K.; Yuki, K.; Yuki, K.; Kibushi, R.; Unno, N. Heat transfer performance of an energy-saving heat removal device with uni-directional porous copper for divertor cooling. *Fusion Eng. Des.* **2018**, *136 Pt A*, 518–521. [CrossRef]
10. Raffray, A.R.; Malang, S.; Wang, X. Optimizing the overall configuration of a He-cooled W-alloy divertor for a power plant. *Fusion Eng. Des.* **2009**, *84*, 1553–1557. [CrossRef]
11. Yoda, M.; Abdel-Khalik, S.I.; Sadowski, D.L.; Mills, B.H.; Rader, J.D. Experimental evaluation of the thermal-hydraulics of helium-cooled divertors. *Fusion Sci. Technol.* **2015**, *67*, 142–157. [CrossRef]
12. Yoda, M.; Abdel-Khalik, S.I. Overview of thermal hydraulics of helium-cooled solid divertors. *Fusion Sci. Technol.* **2017**, *72*, 285–293. [CrossRef]
13. Zhao, B.B.B.; Musa, S.; Abdel-Khalik, S.; Yoda, M. Experimental and numerical studies of helium-cooled modular divertors with multiple jets. *Fusion Eng. Des.* **2018**, *136*, 67–71. [CrossRef]
14. Yokomine, T.; Oohara, K.; Kunugi, T. Experimental investigation on heat transfer of HEMJ type divertor with narrow gap between nozzle and impingement surface. *Fusion Eng. Des.* **2016**, *109*, 1543–1548. [CrossRef]
15. Ji, W.-T.; Jacobi, A.M.; He, Y.-L.; Tao, W.-Q. Summary and evaluation on the heat transfer enhancement techniques of gas laminar and turbulent pipe flow. *Int. J. Heat Mass Transf.* **2017**, *111*, 467–483. [CrossRef]
16. Hermsmeyer, S.; Malang, S. Gas-cooled high performance divertor for a power plant. *Fusion Eng. Des.* **2002**, *61–62*, 197–202. [CrossRef]
17. Sharafat, S.; Mills, A.; Youchison, D.; Nygren, R.; Williams, B.; Ghoniem, N. Ultra low pressure-drop helium-cooled porous-tungsten PFC. *Fusion Sci. Technol.* **2007**, *52*, 559–565. [CrossRef]
18. Sharafat, S.; Aoyama, A.T.; Ghoniem, N.; Williams, B. Design and fabrication of a rectangular he-cooled refractory foam hx-channel for divertor applications. *Fusion Sci. Technol.* **2011**, *60*, 208–212. [CrossRef]
19. Yuki, K.; Kawamoto, M.; Hattori, M.; Suzuki, K.; Sagara, A. Gas-cooled divertor concept with high thermal conductivity porous media. *Fusion Sci. Technol.* **2015**, *61*, 197–202. [CrossRef]
20. Takarazawa, S.; Ushijima, K.; Fleischhauer, R.; Kato, J.; Terada, K.; Cantwell, W.J.; Kaliske, M.; Kagaya, S.; Hasumoto, S. Heat-transfer and pressure drop characteristics of micro-lattice materials fabricated by selective laser metal melting technology. *Heat Mass Transf.* **2022**, *58*, 125–141. [CrossRef]
21. Trevizoli, P.V.; Teyber, R.; da Silveira, P.S.; Scharf, F.; Schillo, S.M.; Niknia, I.; Govindappa, P.; Christiaanse, T.V.; Rowe, A. Thermal-hydraulic evaluation of 3D printed microstructures. *Appl. Therm. Eng.* **2019**, *160*, 113990. [CrossRef]
22. Elkholy, A.; Kempers, R. Enhancement of pool boiling heat transfer using 3D-printed polymer fixtures. *Exp. Therm. Fluid Sci.* **2020**, *114*, 110056. [CrossRef]

23. Guo, Y.; Yang, H.; Lin, G.; Jin, H.; Shen, X.; He, J.; Miao, J. Thermal performance of a 3D printed lattice-structure heat sink packaging phase change material. *Chin. J. Aeronaut.* **2021**, *34*, 373–385. [CrossRef]

24. Hu, X.; Gong, X. Experimental study on the thermal response of PCM-based heat sink using structured porous material fabricated by 3D printing. *Case Stud. Therm. Eng.* **2021**, *24*, 100844. [CrossRef]

25. Liang, D.; He, G.; Chen, W.; Chen, Y.; Chyu, M.K. Fluid flow and heat transfer performance for micro-lattice structures fabricated by Selective Laser Melting. *Int. J. Therm. Sci.* **2022**, *172*, 107312. [CrossRef]

26. Hokamoto, K.; Vesenjak, M.; Ren, Z. Fabrication of cylindrical uni-directional porous metal with explosive compaction. *Mater. Lett.* **2014**, *137*, 323–327. [CrossRef]

27. Ogushi, T.; Chiba, H.; Nakajima, H.; Ikeda, T. Measurement and analysis of effective thermal conductivities of lotus-type porous copper. *J. Appl. Phys.* **2004**, *95*, 5843–5847. [CrossRef]

28. Fiedler, T.; Borovinšek, M.; Hokamoto, K.; Vesenja, M. High-performance thermal capacitors made by explosion forming. *Int. J. Heat Mass Transf.* **2014**, *83*, 366–371. [CrossRef]

29. Yuki, K.; Sato, Y.; Kibushi, R.; Unno, N.; Suzuki, K.; Tomimura, T.; Hokamoto, K. Heat transfer performance of porous copper pipe with uniformly-distributed holes fabricated by explosive welding technique. In Proceedings of the 27th International Symposium on Transport Phenomena (ISTP27), Honolulu, HI, USA, 20–23 September 2016. ISTP27-126.

30. Sato, Y.; Yuki, K.; Abe, Y.; Kibushi, R.; Unno, N.; Hokamoto, K.; Tanaka, S.; Tomimura, T. Heat transfer characteristics of a gas flow in uni-directional porous copper pipes. In Proceedings of the 16th International Heat Transfer Conference (IHTC16), Beijing, China, 10–15 August 2018; pp. 8189–8193.

31. Kibushi, R.; Yuki, K.; Unno, N.; Tanaka, S.; Hokamoto, K. Heat transfer and pressure drop correlations for a gas flow in unidirectional porous copper tubes fabricated by explosive compaction. *Int. J. Heat Mass Transf.* **2022**. submitted.